

Chapter 5

Directed Evolution of P450 BM3 for Ethane Hydroxylation

A. Abstract

In continuing directed evolution of P450 BM3 for small alkane hydroxylation, we developed a high-throughput screen to directly assay for P450 alkane hydroxylation activity. With the use of a pressurizable 96-well reactor, the P450 alkane hydroxylation reaction was conducted in high throughput and the alcohol product was quantified spectroscopically by a coupled enzyme assay utilizing 2,2'-azino-bis(3-ethylbenzthiazoline-6-sulfonic acid) as a horseradish peroxidase (E.C. 1.11.1.7) substrate to detect hydrogen peroxide generated by alcohol oxidase (E.C. 1.1.3.13) oxidation of the product alcohol. Applying this screen to 370 P450 variants generated in our laboratory, we identified variant E31 (WT-A74L-V78I-A82L-A184V-L188W-A328F-A330W) as the best candidate for further engineering. Through subsequent rounds of site-saturation and random mutagenesis, multiple variants supporting 1,700 – 4,000 ethane TONs were identified. Recombination of the identified mutations generated variant E31-D140E-L215P-T436R supporting 5,800 ethane TON. However, none of the BM3 variants were able to produce ethanol or methanol in whole-cell alkane bioconversions using growth-arrested *E. coli* BL21 (DE3) cells. In contrast, CYP153A6, a natural terminal alkane hydroxylase, was able to produce ethanol in whole-cell alkane bioconversions. The inability of BM3 variants to produce ethanol *in vivo* reflects their poor affinity for ethane and indicates they still lag behind a natural P450 alkane hydroxylase in terminal hydroxylation of small alkanes.

B. Introduction

Selective hydroxylation of small alkanes is a long-standing problem for which few practical catalysts are available (1 – 3). The lack of such catalysts that can convert gaseous alkanes into transportable liquid commodities has been a barrier to broader utilization of these resources (4). While this transformation has been achieved only by a limited set of transition-metal – based catalyst systems (5 – 7), a variety of alkane hydroxylases found in alkanotrophic microorganisms support this reaction at ambient conditions using oxygen as the oxidant (8). Unfortunately, since most of these hydroxylases function as a part of a larger enzyme complex and are membrane associated, their potential for industrial applications is limited. For these reasons, we have been engineering well-expressed, soluble, bacterial cytochrome P450 monooxygenases for small gaseous alkane hydroxylation.

Our previous protein engineering efforts have been focused on shifting the substrate specificity of both a self-sufficient P450 fatty acid hydroxylase from *Bacillus megaterium* CYP102A1 (BM3) (9) and a natural P450 medium-chain alkane hydroxylase from *Mycobacterium* sp. HXN-1500 CYP153A6 (A6) (10) to accept smaller alkane substrates. Using a variety of mutagenesis techniques and screening for activity on surrogate substrates such as dimethyl ether (DME) (11), BM3 variants with propane and ethane hydroxylation activity have been generated (12 – 14). Similarly, a variant with improved butane hydroxylation activity was obtained from A6 using random mutagenesis and a growth-based selection (15). While rapid improvements for the activities directly under selection pressure, DME demethylation and terminal butane hydroxylation, were observed in the isolated variants, activity improvements for other substrates varied. In the case of BM3 derived variants, the correlation of DME

demethylation activity with propane hydroxylation activity as measured by turnover number (TON) ($r = 0.74$) was much better than that with ethane hydroxylation activity ($r = 0.52$). Because of this difference in the correlation of activities, only relatively small improvements for ethane hydroxylation were obtained, while a complete shift in substrate specificity from fatty acids to propane was achieved through the application of the DME demethylation screen. Similarly, the growth-based selection used in the *in vivo* directed evolution of A6 also showed a poor predictability for substrates not under selection (15). For example, the isolated variant CYP153A6-BMO1 with improved activity for terminal hydroxylation of butane actually displayed diminished activity for propane hydroxylation.

The importance of the screen or selection to apply the desired selection pressure in directed evolution experiments has been well documented (16 – 18). Therefore, to continue protein engineering of P450s for hydroxylation of even smaller substrates ethane and methane a more suitable screen or selection is necessary. In this chapter, we describe the development of a high-throughput screen for terminal alkane hydroxylation activity using a pressurizable 96-well reactor to conduct the P450 reaction in high throughput and a coupled enzyme assay for colorimetric quantification of the alcohol product. Applying this screen to 370 BM3-derived variants generated in our laboratory, including variants from the alkane hydroxylation lineage (11 – 14), SCHEMA-guided chimeragenesis (19 – 21), and variants evolved for various drug compounds (22 – 23), we identified variant E31 (WT-A74L-V78I-A82L-A184V-L188W-A328F-A330W) as the best candidate for further engineering. Subsequent rounds of random and site saturation mutagenesis with screening for ethane hydroxylation generated variants with 1.5 to 3.3-fold improved activity, demonstrating the efficacy of the screen.

C. Results and Discussion

C.1. *High-throughput ethane hydroxylation assay development*

To apply selection pressure for ethane and methane hydroxylation in our laboratory evolution of P450s, a variety of small molecules was evaluated as surrogate substrates. High throughput screens were developed based on P450 oxidation of dichloromethane, chloromethane, and methanol (see Appendix C). In each instance, activity for these compounds was not a better predictor for ethane hydroxylation activity than DME demethylation. Ultimately, we pursued screening for ethane and methane hydroxylation directly using a pressurizable 96-well reactor system from Symyx (Santa Clara, CA) to conduct the P450 alkane reaction in high throughput. To quantify the alcohol product colorimetrically, the P450 reaction was first coupled to an alcohol oxidase (AO) reaction that converts the alcohol product to one equivalent of hydrogen peroxide and one equivalent of an aldehyde. In a second reaction, horseradish peroxidase (HRP) oxidizes 2,2'-azino-bis(3-ethylbenzthiazoline-6-sulfonic acid) (ABTS) to its green radical cation using the hydrogen peroxide generated by the AO reaction. Thus, quantification of the alcohol product can be achieved spectroscopically with UV/Vis absorbance at 420 nm (24). The substrate scope of this assay is limited by the substrate affinity of AO, which accepts terminal linear alcohols with methanol as its preferred substrate (25).

Figure 5.1 summarizes the reactions of the screen and illustrates the sensitivity of the screen with both ethanol and methanol standards. Following the screening conditions detailed in Chapter 8.E.4, the spectroscopic ($A_{420\text{nm}}$) responses to methanol and ethanol are $0.011 A_{420\text{nm}}/\mu\text{M}$ and $0.005 A_{420\text{nm}}/\mu\text{M}$ and remain linear up to 200 and 600 μM of analyte, respectively. The

difference in alcohol sensitivity reflects the twofold higher substrate affinity (K_M) of AO for methanol compared to ethanol (26).

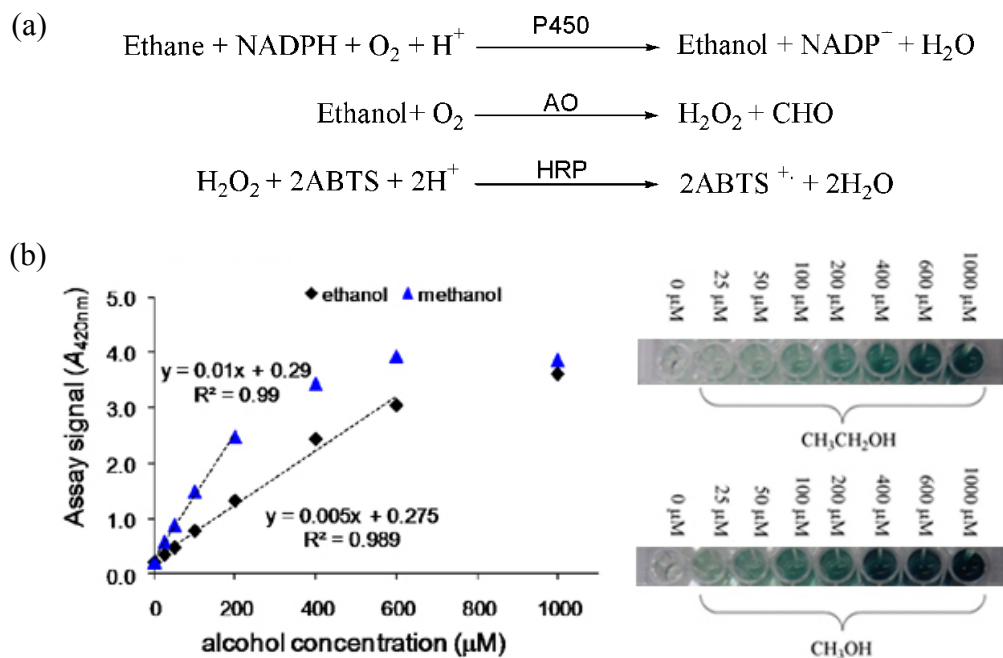


Figure 5.1: The high throughput alkane hydroxylation assay: (a) The coupled enzyme reaction scheme of the assay. (b) Assay sensitivity with methanol and ethanol standards

To validate the assay's ability to accurately quantify P450 ethane hydroxylation reactions, we selected twelve BM3 variants with various ethane activities and tested each variant for ethane hydroxylation as both cell-free extract and purified enzyme. To generate even more variety in ethanol yields, each variant was assayed at three different enzyme concentrations. The resulting ethanol product was quantified by both GC-FID as detailed in Chapter 8.H.2 and the coupled enzymatic assay. Ethanol quantifications were in good agreement between the two methods, with an R^2 of 0.96 based on linear regression of the data, see Figure 5.2. The slope of the regression, 1.20, indicates that the ABTS assay underestimates the ethanol yield in the reactions by 20%. Other than this systematic underestimation of the ethanol yield, the high

throughput colorimetric assay is as precise as GC-FID in evaluating the ethanol yield of P450 reactions.

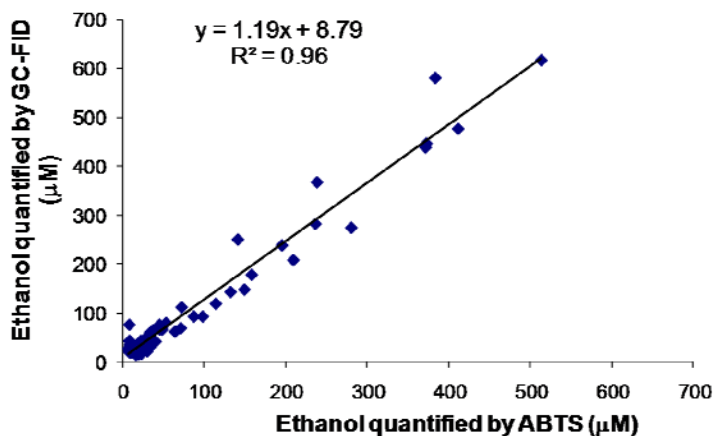


Figure 5.2: Comparison of ethanol quantification by GC-FID with enzymatic colorimetric assay

C.2. *BM3 variants ethane hydroxylation evaluation*

We applied this screen to evaluate BM3 variants that have accumulated in our lab from various projects for ethane and terminal propane hydroxylation activity. Previously, each variant needed to be purified and evaluated individually using GC-FID, which severely limited the number of variants that could be characterized. With the colorimetric assay, hundreds of variants can be evaluated in parallel as cell-free extracts. To this end, we selected 194 BM3 variants from the P450_{PMO} alkane hydroxylation lineage (11 – 14), including a thermostabilized derivative AB2 (P450_{PMO}-C47R-I94K), thermostable chimeras of BM3 with its homologues (20), BM3-derived chimeras displaying a wide range of substrate activities (19, 21), and variants generated during evolution of BM3 for terminal alkane hydroxylation (27). In addition, 88 variants from each of the CRAM and C^{orbit} libraries (Chapter 3) were also selected based on their DME demethylation activities.

A total of 370 variants were tested as cell-free extracts in at least duplicate for both ethane hydroxylation and terminal propane hydroxylation. None of the selected variants supported significant 1-propanol production in the assay ($> 50 \mu\text{M}$ product), while 26 variants were identified to be active for ethane hydroxylation, producing at least $45 \mu\text{M}$ ethanol (see Table 5.1). None of the 55 chimeras of BM3 were found to hydroxylate ethane, which was not surprising, since these enzymes were never selected for this activity. Of the 26 active variants, six were from the PMO lineage: PMO, 7-7, 1-3, 53-5H, 35E11, and AB2, supporting ethane TON ranging from 440 to 1,260 in cell-free extracts. Two ethane-hydroxylating variants isolated from the reduced CASTing library detailed in Chapter 3, WT-A82L-A328V and WT-A82L-A328L, were also identified by the screen.

In addition to these known ethane-hydroxylating variants, WT-V78F-A82S-A328F and WT-V78T-A82G-A328L, which were generated by grafting only the active site mutations of variants 53-5H (14) and 77-H9 (14) onto wild-type BM3, were also found to support 180 and 210 ethane TONs, respectively. Although 53-5H shows a threefold increase in ethane TON as compared to WT-V78F-A82S-A328F, both variants produce the same amount of ethanol, since the improvement in activity was offset by a decrease in protein expression. The remaining 16 variants were identified from the CRAM (13) and C^{orbit} (3) libraries as detailed in Chapter 3.

Table 5.1: Ethane hydroxylating BM3 variants identified by the high-throughput screen

Variant source	Variant	Assay signal ^a (A_{420nm})	Ethanol product ^a (μ M)	Ethane TON ^a	Standard error
PMO lineage	1-3	0.64	81	1,070	150
PMO lineage	7-7	1.31	229	1,260	50
PMO lineage	AB2	0.93	154	1,110	180
PMO lineage	PMO	1.00	155	940	60
PMO lineage	53-5H	0.46	50	530	20
PMO lineage	35-E11	0.41	45	440	70
Reduced CASTing Library	WT-A82L-A328V	0.76	109	390	50
Reduced CASTing Library	WT- A82L-A328L	0.72	73	220	20
WT-779H	WT-V78T-A82G-A328L	0.58	52	210	60
WT-53-5H	WT-V78F-A82L-A328V	0.47	45	180	40
CRAM library	CB8	0.52	49	300	20
CRAM library	CD7	0.55	54	410	60
CRAM library	CG2	0.74	92	610	100
CRAM library	CE4	0.58	61	630	20
CRAM library	CA3	0.60	64	670	100
CRAM library	CA4	0.55	54	760	110
CRAM library	E78	0.84	111	930	40
CRAM library	E41	0.73	90	960	140
CRAM library	E30	0.86	114	980	90
CRAM library	E66	0.94	131	1,020	70
CRAM library	CF2	1.27	195	1,070	140
CRAM library	E32	1.00	142	1,350	20
CRAM library	E31	1.28	198	1,860	30
Corbit library	OD7	0.67	77	670	70
Corbit library	OD2	0.55	55	500	80
Corbit library	OE5	0.45	45	250	40

^a Ethane reactions contained ca. 100 nM protein, alkane saturated potassium phosphate buffer, and an NADPH regeneration system containing 100 μ M NADP⁺, 2 U/mL isocitrate dehydrogenase, and 10 mM isocitrate (see Chapter 8.E.4 for experimental details). TON determined as nmol product/nmol enzyme.

From these 26 variants, we selected variant E31 (WT-A74L-V78I-A82L-A184V-L188W-A328F-A330W) as the parent for further directed evolution for ethane hydroxylation. It not only displayed the highest ethane TON in the cell-free extract assay, but also had a higher thermostability than wild-type BM3 with a half-denaturation temperature (T_{50}), the temperature at which the enzyme retains 50% of its activity after a 15 minute incubation, of 56.2 °C compared to 54.5 °C for wild-type BM3. In comparison, the thermostabilities of other candidates from the PMO lineage with comparable $A_{420\text{nm}}$ such as 7-7 ($T_{50} = 44.2$ °C) or AB2 ($T_{50} = 48.9$ °C) were much lower.

To further validate the high-throughput ethane hydroxylation screen, we applied the assay across a 96-well plate containing *E. coli* cultures expressing variant E31. Using 20 μL of cell-free extract in the P450 reaction, which corresponds to ca. 120 nM of enzyme, an average TON of 1,830 was obtained with a coefficient of variance (CV) of 33% (see Figure 5.3 (a)). Increasing the enzyme loading of the reaction by using 40 μL of cell-free extract marginally increased the amount of ethanol product (from 230 μM to 310 μM) and resulted in 1,230 TON (CV of 24%). This decrease in TON with increased enzyme loading indicates that the P450 reaction with 40 μL cell-free extract is no longer limited by enzyme activity but rather by the depletion of a reactant, most likely oxygen (11). Therefore, the improvement in CV is merely an artifact of the reaction reaching a saturating limit rather than a systematic improvement of assay precision. Based on these results, 20 μL of cell-free extract were used in P450 reactions for the screening of E31 and subsequent mutant libraries.

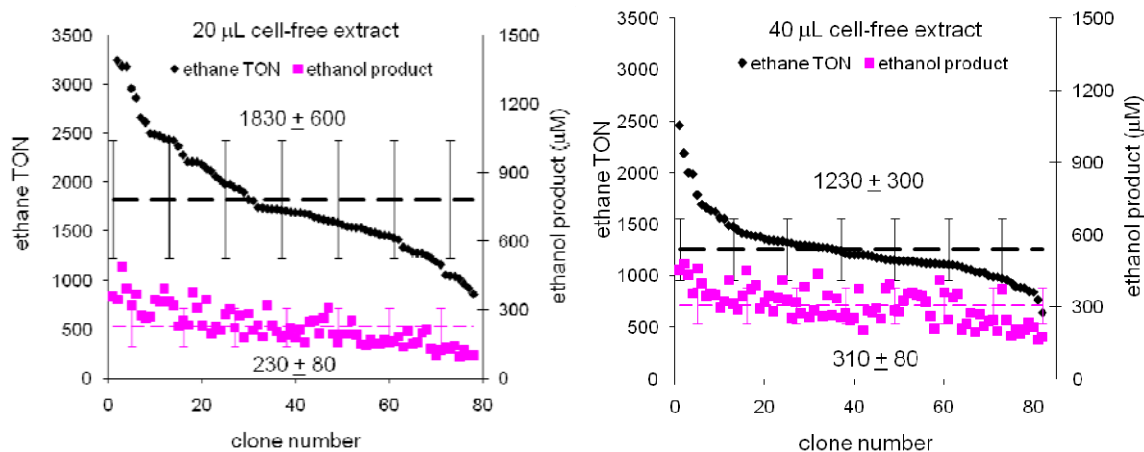


Figure 5.3: Ethane hydroxylation validation with monoclonal E31 plate: (a) 20 µL cell-free extract in 500 µL reaction (ca. 120 nM P450), (b) 40 µL cell-free extract in 500 µL reaction (ca. 240 nM P450)

C.3. Random mutagenesis of variant E31 for ethane hydroxylation

Following validation of the high-throughput ethane hydroxylation screen with the monoclonal 96-well plate of variant E31, both random mutagenesis and active site saturation mutagenesis were pursued to improve ethane hydroxylation activity. For random mutagenesis, an error-prone PCR library using the gene encoding variant E31 as template was constructed with a commercial mutagenic polymerase, Mutazyme II[®]. Following the supplied protocols, a library with an average nucleotide substitution rate of 3.7/protein was obtained using 100 ng of template DNA. From screening 2,640 variants of this library for ethane hydroxylation activity, we obtained two variants, 24F8 (E31-E140D, L215P, P454S) and 22H11 (E31-D222E, A289E) with 1.6- and 1.5-fold increased ethane TON, respectively.

Surprisingly, the ethane TON of the purified enzymes was found to be significantly lower than the observed TON in the cell-free extract screening (see Table 5.2). This decrease in enzyme activity with purification contradicts our previous experience, in which propane TON is generally higher with purified enzymes compared to cell-free extracts (11). The most likely culprit for this difference is the reduced accuracy of P450 protein concentration determination in

cell-free extract as compared to purified enzymes. To expedite the CO-binding assay on a 96-well plate scale, the reducing agent, sodium hydrosulfite, is added to the enzyme solution before exposure to carbon monoxide (28). Since sodium hydrosulfite is unstable and reacts with oxygen to generate superoxide and hydrogen peroxide, which are deleterious to both the P450 and its heme prosthetic group (29), the inevitable protein/heme degradation may result in underestimation of the actual amount of P450 used in the screening reactions.

Table 5.2: Ethane TON of select variants as cell-free extract and purified enzyme

Variant	Ethane TON			
	Cell-free extract ^a	CV (%) ^b	Purified enzyme ^a	CV (%) ^b
E31	1,830	32.8	1,200	15.4
22H11	2,200	27.3	1,800	14.9
24F8	3,400	24.2	1,900	13.2

^a TON determined as nmol product/nmol enzyme. Ethane reactions contained ~ 100 nM protein, alkane saturated potassium phosphate buffer, and an NADPH regeneration system containing 100 μ M NADP⁺, 2 U/mL isocitrate dehydrogenase, and 10 mM isocitrate (see Chapter 8.E.4 for experimental details).

^b CV determined as the ratio of the standard error over the mean determined from four replicate reactions.

All five mutations found in these two variants occur at surface-exposed residues outside of the active site. Mutations L215P and D222E are located in the G helix, adjacent to residues that are part of substrate recognition site three of type II P450s (30). However, the side chains of these two residues are oriented away from the active site and do not appear to interact with the residues known to alter P450 substrate specificity. While the L215P mutation should disrupt the packing of this helix, rationalizing of how such an effect would lead to improved activity is difficult.

Due to the high mutation rate of the error-prone PCR library, these variants are carrying multiple mutations, which are unlikely to all be beneficial. To eliminate potential neutral and deleterious mutations, a recombination library allowing all five mutations and the corresponding wild-type amino acid at each position were constructed using splicing by overlap extension

polymerase chain reaction (SOE-PCR) (31). From screening 90 clones of this library with 32 unique members (94% completeness), we found two variants with improved ethane hydroxylation activity compared to variant 24F8. These two variants, RA1 (E31-D140E-L215P-D222E) and RD2 (E31-D140E-L215P), supported 2,100 and 2,200 ethane TON, respectively. Variant RD2 is variant 24F8 without the P454S mutation, which appears to be deleterious for ethane hydroxylation activity. Variant RA1 recombined the two mutations of RD2 with D222E from 22H11, this latter mutation also appears to be deleterious since the activity of RA1 is diminished compared to RD2. The thermostabilities of variants 24F8, RA1, and RD2 were determined to select a parent for the next library. Surprisingly, the T_{50} s of all three variants, 49 – 51 °C, were significantly lower than that of the parent, variant E31 (56 °C). This large decrease in thermostability was reminiscent of the introduction of the L188P mutation in the PMO evolutionary lineage ($\Delta T_{50} = -3$ °C), which also replaced a leucine in a α -helix with a proline.

Without significant differences in thermostability between these variants, we constructed a second error-prone PCR library with the gene encoding RD2 as the template using *Taq* polymerase (32). From screening 2,640 members of this library with an average nucleotide substitution rate of 4.3/protein, variant 20D4 (RD2-D432G) was found with a 1.8-fold improvement in ethane hydroxylation activity. The D432G mutation occurs in the β 4 sheet, close to G443A mutation identified in the PMO evolutionary lineage (33). This mutation would disrupt existing hydrogen bonds of D432 with Y429, E430, and E442, which could destabilize the folding of the beta-sheet. The importance of this beta-sheet structure for P450 function lies in E435, located at the bend of the sheet, which has been shown to participate in the proton

transport chain (34). In these two rounds of random mutagenesis, an overall 3.3-fold increase in ethane TON was achieved from variant E31 (1,200 TON) to variant 20D4 (4,000 TON).

C.4. Active site site-saturation mutagenesis of variant E31 for ethane hydroxylation

In addition to the random mutagenesis, ten active site residues of variant E31 were also targeted for site-saturation mutagenesis. Because variant E31 was isolated from the CRAM computationally designed library, which mutated ten active site residues allowing two amino acids at each position, it already contained seven active site mutations: A74L, V78I, A82L, A184V, L188W, A328F, and A330W. Instead of mutating many of these previously targeted residues again, we selected the targets for mutagenesis accounting for the sequence consensus of the ethane hydroxylation variants of the CRAM library. The ethane-hydroxylating CRAM variants displayed significant amino acid preference (> 70% representation) for F at position 87, L at position 75, W at position 188, and W at position 330. Therefore, these four positions were not mutated. Thus the ten residues targeted for saturation mutagenesis were composed of the six remaining targets from the computationally-guided libraries, A74, L75, V78, A82, A184, and A328, and residues in regions of the active site not mutated in E31, A263, I264, T436, and L437. Residues A263 and I264 are located in the I helix which constitutes the surface of the active site opposite to the B' helix that contains residues 74, 75, 78, and 82. T436 and L437 are in the β 4 sheet, which contains mutations previously found to be beneficial for small alkane hydroxylation in the PMO evolutionary lineage (33).

These ten site-saturation libraries were constructed with SOE-PCR and screened to 94% completeness for ethane hydroxylation. Differences between the fraction of folded variants of these libraries and equivalent libraries constructed with wild-type BM3 revealed a decreased

mutational tolerance at these residues of E31 compared to wild-type BM3. Of the six libraries constructed with both enzymes (A74, L75, V78, A184, and A328), the fraction of folded variants decreased from an average of 0.95 with wild-type BM3 to 0.67 with variant E31. The single largest decrease occurred at position A82, for which the wild-type BM3 tolerated all possible mutations, but the equivalent E31 library contained only 36% of folded variants. Since both enzymes have similar thermostabilities, this decrease in mutational tolerance indicates that the active site of E31 is much smaller or more rigid than wild-type BM3, such that many more mutations result in steric clashes with neighboring residues.

From these site-saturation libraries, we identified four variants with mutations L74R, I78W, T436L, and T436R, supporting 1,700 – 2,600 ethane TON. Of the libraries targeting the six residues that were previously subjected to mutagenesis, only two (L74R and I78W) of the 120 total possible mutations were found to be beneficial. The lack of beneficial mutations at residues L82, V184, and F328 implies that these amino acids are the best solutions for ethane hydroxylation activity in the context of the remaining E31 mutations. Two of the four beneficial mutations introduced a positively charged arginine into the active site. The introduction of amino acids with charged side-chains into the active site also occurred in the PMO lineage and has been hypothesized to separate the active site volume into distinct pockets (33). The other two beneficial mutations, I78W and T436L, introduced bulkier amino acids, continuing the trend of volume-reducing mutations.

C.5. Recombination of active site mutations with mutations from error-prone PCR libraries

Using variant RD2 as the parent, the beneficial mutations for ethane hydroxylation identified from site-saturation mutagenesis and the second round of random mutagenesis were

recombined. Variant RD2 was selected as the parent, since its mutations have already been shown to be beneficial through a prior round of recombination. In addition, its mutations E140D and L215P are distant from the active site, which should reduce the probability of the mutations interacting during recombination. In contrast, the mutation identified in the second round of random mutagenesis, D432G, lies in close proximity to active site residue T436. By including this mutation in the recombination library, this residue was allowed to revert to the wild-type amino acid, which would avoid potential conflicts with mutations at T436. Starting with RD2, a recombination library allowing mutations L74R, I78W, T436L, T436R, D432G, and the corresponding wild-type amino acid at each position was constructed using SOE-PCR and screened for ethane hydroxylation to 94% completeness. From this library, we identified variant RD2-T436R (E31-D140E-L215P-T436R), supporting 5,800 ethane TON, as the most active variant.

C.6. Whole-cell alkane bioconversions

Having increased the ethane TON nearly fivefold from E31 to E31-D140E-L215P-T436R, we next tested these variants for their ability to produce methanol in *in vitro* methane hydroxylation reactions. None of variants generated from E31 were able to produce detectable amounts of methanol ($> 2 \mu\text{M}$) in these reactions. From our previous work with P450_{PMO} (Chapter 2) and CYP153A6 (Chapter 4), we demonstrated that the alcohol yield of P450 whole-cell bioconversions supported with a continuous supply of alkane and oxygen can reach up to 15 mM of alcohols (12). Since the product yields of these whole-cell bioconversions are generally much higher than those obtained in *in vitro* P450 reactions (0.5 – 2 mM), we assayed several of

the ethane hydroxylation variants in whole-cell bioconversions for small alkane hydroxylation, including methane.

Using growth and expression conditions outlined in Chapter 8.K.1, propane bioconversions were first conducted with selected variants with PMO and CYP153A6 as controls to verify their viability in whole-cell bioconversions and to monitor the background ethanol fermentation under reaction conditions (see Figure 5.4). All six variants were able to produce propanol with activities ranging from 19 to 120 U/ μ mol P450, where 1 U = 1 μ mol product/min. While we did not explicitly evolve variants RD2, 20D4, and RD2-T436R for improved propane hydroxylation activity, their *in vivo* propane hydroxylation activities are correlated with their *in vitro* ethane hydroxylation activities. The best ethane-hydroxylating variant RD2-T436R was nearly sixfold more productive than PMO for *in vivo* propane hydroxylation. GC-FID analysis of these propane bioconversions showed only an average of 52 ± 10 μ M of ethanol was produced, which indicates minimal background ethanol fermentation.

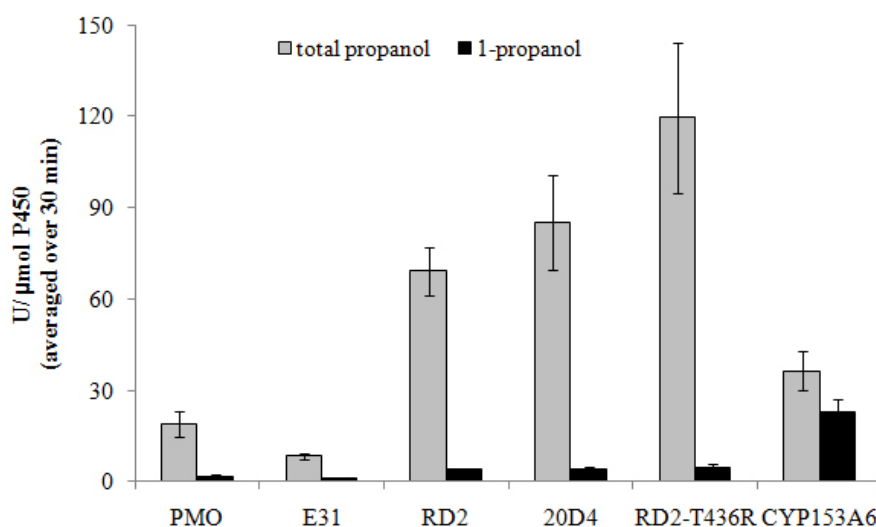


Figure 5.4: Whole-cell propane bioconversion of select P450 variants, following protocols outlined in Chapter 8.K.1

When the alkane source of the bioconversions was switched from propane to ethane with all other conditions unchanged, none of the cells containing BM3-derived variants were found to produce ethanol above background levels. The only P450 with *in vivo* ethane hydroxylation activity was CYP153A6, with a yield of 340 ± 80 μM ethanol after 30 minutes, corresponding to an activity of 8.7 U/ μmol P450. None of the P450s were able to produce detectable amounts of methanol in methane bioconversions.

The lack of *in vivo* ethane hydroxylation activity of BM3 variants with *in vitro* ethane hydroxylation activity is perplexing considering that the same variants were able to produce propanol under identical conditions. This discrepancy may be due to the presence of other P450 substrates such as indole (35 – 36) or endogenous fatty acids that compete with the alkane during the whole-cell reactions but are absent during the *in vitro* reactions. The presence of the indole reaction is readily apparent by the visible formation of indigo over the course of the whole-cell reactions and the presence of other endogenous substrates is suggested by an increased rate of cofactor consumption when purified enzymes are assayed in the presence of cell lysate (data not shown).

D. Conclusion and Future Directions

Using a high throughput screen for P450 ethane hydroxylation, we have found variants with improved *in vitro* ethane hydroxylation through both random and site-saturation mutagenesis. However, the inability of even the most active variant, RD2-T436R, to hydroxylate ethane in whole-cell bioconversions reflects a poor affinity for ethane and highlights the gap between our current BM3 variants and a natural P450 terminal alkane hydroxylase, CYP153A6.

Although the lack of *in vivo* ethane hydroxylation is a discouraging outcome in measuring the progress of BM3 evolution, it does not eliminate the possibility that a BM3-derived variant can support *in vivo* ethane or methane hydroxylation. Iterative rounds of random and target mutagenesis that were applied in this chapter can be continued to further improve the *in vitro* ethane hydroxylation activity. However, CYP153A6, which already hydroxylates ethane as a natural, promiscuous function and supports ethane whole-cell bioconversion may be a better starting point for the engineering of a P450-based methane monooxygenase.

The drawbacks of engineering CYP153A6 are (1) it is a type I P450 with its reductase components expressed as separate enzymes, and (2) no crystal structure has been solved for any of the CYP153 family members. For these reasons, we initially pursued the *in vivo* selection-based evolution of CYP153A6 as described in Chapter 4. However, it is clear that the growth-based selection is inefficient at applying selection pressure to improve enzyme activity, as plasmid and strain adaptations were obtained with equal frequency as enzyme mutations. To engineer CYP153A6 for ethane and methane hydroxylation activity, a suitable high throughput screen is necessary. One option is to apply the ethane/methane hydroxylation screen described in this chapter and supply the reductase components through either co-expression or addition as purified enzymes. Another applicable screen is the dehalogenation of iodomethane, which releases formaldehyde that can be quantified colorimetrically by Purpald®.

The lack of a CYP153A6 crystal structure is perhaps a bigger barrier for protein engineering, since the application of the many targeted mutagenesis techniques described in Chapter 3 would not be possible. While a homology model of CYP153A6 based on the CYP101 structure is available (10), its accuracy is questionable since the bound substrate, octane, is

largely solvent-exposed in the model. Therefore, solving the crystal structure of CYP153A6 or obtaining a suitable homology model should be pursued with a high priority. Until such structural information becomes available, random mutagenesis is the only reasonable approach.

E. References

1. Labinger, J. A., and Bercaw, J. E. (2002) Understanding and exploiting C-H bond activation, *Nature* 417, 507-514.
2. Shul'pin, G. B., Suss-Fink, G., and Shul'pina, L. S. (2001) Oxidations by the system "hydrogen peroxide-manganese(IV) complex-carboxylic acid" Part 3. Oxygenation of ethane, higher alkanes, alcohols, olefins and sulfides, *J. Mol. Catal. A-Chem.* 170, 17-34.
3. Yamanaka, I., Hasegawa, S., and Otsuka, K. (2002) Partial oxidation of light alkanes by reductive activated oxygen over the (Pd-black + VO(acac)₂/VGCF) cathode of H₂-O₂ cell system at 298 K, *Appl. Catal. A-Gen.* 226, 305-315.
4. Arakawa, H., Aresta, M., Armor, J. N., Barteau, M. A., Beckman, E. J., Bell, A. T., Bercaw, J. E., Creutz, C., Dinjus, E., Dixon, D. A., Domen, K., DuBois, D. L., Eckert, J., Fujita, E., Gibson, D. H., Goddard, W. A., Goodman, D. W., Keller, J., Kubas, G. J., Kung, H. H., Lyons, J. E., Manzer, L. E., Marks, T. J., Morokuma, K., Nicholas, K. M., Periana, R., Que, L., Rostrup-Nielson, J., Sachtler, W. M. H., Schmidt, L. D., Sen, A., Somorjai, G. A., Stair, P. C., Stults, B. R., and Tumas, W. (2001) Catalysis research of relevance to carbon management: Progress, challenges, and opportunities, *Chem. Rev.* 101, 953-996.
5. Mizuno, N., Ishige, H., Seki, Y., Misono, M., Suh, D. J., Han, W., and Kudo, T. (1997) Low-temperature oxygenation of methane into formic acid with molecular oxygen in the presence of hydrogen catalysed by Pd_{0.08}Cs_{2.5}H_{1.34}PVMo₁₁O₄₀, *Chemical Communications*, 1295-1296.
6. Periana, R. A., Taube, D. J., Gamble, S., Taube, H., Satoh, T., and Fujii, H. (1998) Platinum catalysts for the high-yield oxidation of methane to a methanol derivative, *Science* 280, 560-564.
7. Ushikubo, T. N., H.; Koyasu, Y.; Wajiki, S. . (1995) (Pat., U. S., Ed.).
8. van Beilen, J. B., and Funhoff, E. G. (2007) Alkane hydroxylases involved in microbial alkane degradation, *Applied Microbiology and Biotechnology* 74, 13-21.
9. Fulco, A. J. (1991) P450BM-3 and other inducible bacterial P450 cytochromes - biochemistry and regulation, *Annu. Rev. Pharmacol. Toxicol.* 31, 177-203.
10. Funhoff, E. G., Bauer, U., Garcia-Rubio, I., Witholt, B., and van Beilen, J. B. (2006) CYP153A6, a soluble P450 oxygenase catalyzing terminal-alkane hydroxylation, *Journal of Bacteriology* 188, 5220-5227.
11. Peters, M. W., Meinhold, P., Glieder, A., and Arnold, F. H. (2003) Regio- and enantioselective alkane hydroxylation with engineered cytochromes P450 BM-3, *J. Am. Chem. Soc.* 125, 13442-13450.
12. Fasan, R., Chen, M. M., Crook, N. C., and Arnold, F. H. (2007) Engineered alkane-hydroxylating cytochrome P450(BM3) exhibiting natively catalytic properties, *Angewandte Chemie-International Edition* 46, 8414-8418.

13. Glieder, A., Farinas, E. T., and Arnold, F. H. (2002) Laboratory evolution of a soluble, self-sufficient, highly active alkane hydroxylase, *Nat. Biotechnol.* *20*, 1135-1139.
14. Meinhold, P., Peters, M. W., Chen, M. M. Y., Takahashi, K., and Arnold, F. H. (2005) Direct conversion of ethane to ethanol by engineered cytochrome P450BM3, *Chembiochem* *6*, 1765-1768.
15. Koch, D. J., Chen, M. M., van Beilen, J. B., and Arnold, F. H. (2009) *In vivo* evolution of butane oxidation by terminal alkane hydroxylases AlkB and CYP153A6, *Applied and Environmental Microbiology* *75*, 337-344.
16. Arnold, F. H. (1998) Design by directed evolution, *Accounts Chem. Res.* *31*, 125-131.
17. You, L., and Arnold, F. H. (1996) Directed evolution of subtilisin E in *Bacillus subtilis* to enhance total activity in aqueous dimethylformamide, *Protein Eng.* *9*, 77-83.
18. Zhao, H. M., and Arnold, F. H. (1997) Combinatorial protein design: Strategies for screening protein libraries, *Curr. Opin. Struct. Biol.* *7*, 480-485.
19. Landwehr, M., Carbone, M., Otey, C. R., Li, Y. G., and Arnold, F. H. (2007) Diversification of catalytic function in a synthetic family of chimeric cytochrome P450s, *Chem. Biol.* *14*, 269-278.
20. Li, Y. G., Drummond, D. A., Sawayama, A. M., Snow, C. D., Bloom, J. D., and Arnold, F. H. (2007) A diverse family of thermostable cytochrome P450s created by recombination of stabilizing fragments, *Nat. Biotechnol.* *25*, 1051-1056.
21. Otey, C. R., Landwehr, M., Endelman, J. B., Hiraga, K., Bloom, J. D., and Arnold, F. H. (2006) Structure-guided recombination creates an artificial family of cytochromes P450, *PLoS Biol.* *4*, 789-798.
22. Landwehr, M., Hochrein, L., Otey, C. R., Kasrayan, A., Backvall, J. E., and Arnold, F. H. (2006) Enantioselective alpha-hydroxylation of 2-arylacetic acid derivatives and buspirone catalyzed by engineered cytochrome P450BM-3, *J. Am. Chem. Soc.* *128*, 6058-6059.
23. Otey, C. R., Bandara, G., Lalonde, J., Takahashi, K., and Arnold, F. H. (2006) Preparation of human metabolites of propranolol using laboratory-evolved bacterial cytochromes P450, *Biotechnology and Bioengineering* *93*, 494-499.
24. Childs, R. E., and Bardsley, W. G. (1975) Steady-state kinetics of peroxidase with 2,2'-azido-di-(3-ethylbenzthiazoline-6-sulphonic acid) as chromogen, *Biochem. J.* *145*, 93-103.
25. Patel, R. N., Hou, C. T., Laskin, A. I., and Derelanko, P. (1981) Microbial oxidation of methanol - properties of crystallized alcohol oxidase from a yeast, *Pichia Sp.*, *Arch. Biochem. Biophys.* *210*, 481-488.
26. Kato, N., Omori, Y., Tani, Y., and Ogata, K. (1976) Alcohol oxidases of *Kloeckera Sp.* and *Hansenula-polymorpha* - catalytic properties and subunit structures, *Eur. J. Biochem.* *64*, 341-350.

27. Meinhold, P., Peters, M. W., Hartwick, A., Hernandez, A. R., and Arnold, F. H. (2006) Engineering cytochrome P450BM3 for terminal alkane hydroxylation, *Advanced Synthesis & Catalysis* 348, 763-772.
28. Otey, C., (Ed.) (2003) *High-throughput carbon monoxide binding assay for cytochrome P450*, Vol. 230, Humana Press Inc., Totowa, NJ.
29. Guengerich, F. P. (1978) Destruction of heme and hemoproteins mediated by liver microsomal reduced nicotinamide adenine-dinucleotide phosphate-cytochrome p-450 reductase, *Biochemistry* 17, 3633-3639.
30. Pylypenko, O., and Schlichting, I. (2004) Structural aspects of ligand binding to and electron transfer in bacterial and fungal P450s, *Annu. Rev. Biochem.* 73, 991-1018.
31. Kunkel, T. A. (1985) Rapid and efficient site-specific mutagenesis without phenotypic selection, *Proceedings of the National Academy of Sciences of the United States of America* 82, 488-492.
32. Cadwell, R. C., and Joyce, G. F. (1994) Mutagenic PCR *PCR-Methods Appl.* 3, S136-S140.
33. Fasan, R., Meharena, Y. T., Snow, C. D., Poulos, T. L., and Arnold, F. H. (2008) Evolutionary history of a specialized P450 propane monooxygenase, *Journal of Molecular Biology* 383, 1069-1080.
34. Schlichting, I., Berendzen, J., Chu, K., Stock, A. M., Maves, S. A., Benson, D. E., Sweet, B. M., Ringe, D., Petsko, G. A., and Sligar, S. G. (2000) The catalytic pathway of cytochrome P450cam at atomic resolution, *Science* 287, 1615-1622.
35. Li, Q. S., Schwaneberg, U., Fischer, P., and Schmid, R. D. (2000) Directed evolution of the fatty-acid hydroxylase P450BM-3 into an indole-hydroxylating catalyst, *Chemistry-a European Journal* 6, 1531-1536.
36. Whitehouse, C. J. C., Bell, S. G., Tufton, H. G., Kenny, R. J. P., Ogilvie, L. C. I., and Wong, L. L. (2008) Evolved CYP102A1 (P450(BM3)) variants oxidise a range of non-natural substrates and offer new selectivity options, *Chemical Communications*, 966-968.